

Immobilized Poly(anthraquinones) for Electrochemical Energy Storage Applications: Structure-Property Relations

Dominik Wielend,^{*[a]} Yolanda Salinas,^[b] Felix Mayr,^[a, c] Matthias Bechmann,^[d] Cigdem Yumusak,^[a, e] Helmut Neugebauer,^[a] Oliver Brüggemann,^[b] and Niyazi Serdar Sariciftci^[a]

The majority of energy storage devices like batteries, fuel cells or electrolyzers require heterogeneous electrodes. Immobilization of redox-active organic molecules by a polymeric approach seems to be a promising route towards organic electrodes for electrocatalytic energy storage or in batteries. Although numerous reports on synthesis and application of new poly-anthraquinones exist, a universal guideline or tool for selection of the best polymer, concerning several energy storage applications, is still underdeveloped. Moving into the direction

of developing such a tool, we have selected and synthesized three poly(anthraquinones). NMR, FTIR, UV-Vis, TGA, contact angle measurement and SEM revealed certain structure-property trends, which can be correlated with the performance in the electrochemical investigation. The insights gained within this work demonstrate correlations between the FTIR frequencies and the electrochemical reduction potential, as well as between the polymer hydrophobicity and the electrochemical performance.

Introduction

Nowadays the majority of the technologically used electrode materials for energy storage like batteries or electrolyzers are based on inorganic materials.^[1–3] Besides the ecological or toxicological reasons, for some applications like portable devices also the weight is crucial.^[4–8] On the way towards

organic based materials, anthraquinones (AQ) are one of the most studied group^[9,10] for usage in energy storage applications like as organic electrode material for metal-ion batteries,^[6,11–13] redox-flow batteries,^[14,15] supercapacitors,^[16,17] pseudocapacitive ion separation,^[18] electrochemical carbon dioxide (CO₂) capture,^[19–21] the electrocatalytic oxygen (O₂) reduction reaction (ORR)^[22–24] or even medical applications.^[25] Except for redox-flow batteries heterogeneous redox-active materials are required.

One of the bottle-necks for broad utilization of AQ-based energy storage devices is the heavy reductive dissolution of the reduced AQ species in numerous solvents, which limits the long-term stability.^[21,26,27] To overcome this problem, several approaches have been explored throughout the last decades: One non-reacting approach was mixing of the redox-active molecules with carbonaceous materials for high integral conductivity as composite^[28,29] or by a more specific pathway through the non-covalently binding of AQ units to carbon nanotubes.^[30–32] The second approach was based on immobilizing the redox-active units in polymeric way, which can be split into two cases. One case was the use of conductive polymers itself like for example polythiophenes or polypyrrole, which are mostly insoluble after polymerization.^[33] Exactly this insolubility can be beneficial if directly electropolymerized onto the electrode of choice as reported for battery applications^[34,35] as well as for electrocatalysis,^[36,37] also extensively by our group.^[38–41]

Besides using a conductive polymer, also the approach of immobilizing the redox-active units onto non-conductive polymeric chains are reported for decades.^[25,42,43] In this report different polymeric approaches involving separated synthesis and film-casting steps are compared. Although the polymeric backbone itself may not be electrically conductive, by optimizing the mixture with carbonaceous materials or operating as thin-film electrodes allow the facile use of such polymers for energy storage application, which was also reviewed


[a] D. Wielend, F. Mayr, Dr. C. Yumusak, Dr. H. Neugebauer, Prof. Dr. N. S. Sariciftci
Linz Institute for Organic Solar Cells (LIOS)
Institute of Physical Chemistry
Johannes Kepler University Linz
Altenberger Straße 69
4040 Linz, Austria
E-mail: dominik.wielend@jku.at


[b] Dr. Y. Salinas, Prof. Dr. O. Brüggemann
Institute of Polymer Chemistry (ICP)
Johannes Kepler University Linz
Altenberger Straße 69
4040 Linz, Austria

[c] F. Mayr
Institute of Applied Physics
Johannes Kepler University Linz
Altenberger Straße 69
4040 Linz, Austria

[d] Dr. M. Bechmann
Institute of Organic Chemistry
Johannes Kepler University Linz
Altenberger Straße 69
4040 Linz, Austria

[e] Dr. C. Yumusak
Materials Research Centre, Faculty of Chemistry
Brno University of Technology
Purkyňova 118
612 00 Brno, Czech Republic

 Supporting information for this article is available on the WWW under <https://doi.org/10.1002/celec.202101315>

 © 2021 The Authors. ChemElectroChem published by Wiley-VCH GmbH. This is an open access article under the terms of the Creative Commons Attribution License, which permits use, distribution and reproduction in any medium, provided the original work is properly cited.

recently.^[25,44] Even if a few of the materials mentioned were already reported also for electrocatalysis,^[45] the majority was only explored as battery electrode material.

In order the gain in-depth knowledge on why or which polymerization type is beneficial for which kind of energy storage application, three AQ-based polymers were chosen, synthesized and their surface-related properties thoroughly investigated, as well as their electrochemical performance under different conditions. Therefore poly(diallyldimethyl ammonium sulfonic acid anthraquinone) (PDDA-SAQ) was chosen as electrostatically bound poly(ionic liquid).^[45,46] The covalently polymerized poly-1,4-anthraquinone (P14AQ)^[26,47,48], having a π -conjugated backbone structure, was also chosen in direct comparison to poly(2-vinylanthraquinone) (PVAQ),^[49] which consists of a polyethylene polymer backbone with pendant AQ units.

The main goal here is to compare the spectroscopic properties of the resulting polymers with those related to surface and electrochemistry and thereof derive structure-property relations, to guide future synthetic directions of polymer immobilization approaches.

Results and Discussion

In order to compare different types of immobilization of redox-active anthraquinone moieties in polymeric structures, the three polymers PDDA-SAQ, P14AQ and PVAQ were successfully synthesized, according to reported and adapted procedures^[26,45,47,49,50] (see experimental section for all details).

P14AQ and PVAQ consist of covalently linked anthraquinone units whereas in case of PDDA-SAQ the anionic anthraquinone units are bound ionically to the positively charged polymer backbone structure. After drying, all three synthesized polymers had a pale-yellow appearance as powder, as can be seen from

Figure 1. Particularly, PDDA-SAQ was the only polymer not fully soluble in any solvent, thus it was suspended and swollen in *N,N*-dimethyl formamide (DMF) for further processing. However, no solution-based characterization such as ¹H nuclear magnetic resonance (NMR) spectroscopy and UV-Vis absorption of polymer solution could be performed for PDDA-SAQ. In good agreement to the literature report,^[26] P14AQ is the only polymer that can form a freestanding film with intensive yellow colour.

Spectroscopic Characterization

¹H NMR, together with UV-Vis and FTIR spectroscopy were utilized to confirm the chemical structure of the prepared polymers. For P14AQ and PVAQ, polymer formation is clearly indicated by the different chemical shifts and broadening of the signals in the ¹H NMR spectra as compared to the respective monomers (see Figure S1 in Supporting Information). The shape along with the peak ratio of P14AQ was determined to be exactly like reported by Li *et al.*^[48]

Diffusion ordered spectroscopy (DOSY) calculates diffusion coefficients D_i for individual resonances in NMR spectra.^[51] As these coefficients are related to the hydrodynamic radius of the solute(s) it can be applied to discriminate between different sizes and shapes of polymers, or to separate NMR resonances of different components of molecular mixtures. This allows the separation of resonances of polymers and residual monomeric species in the NMR spectra.

In this work, DOSY was used to separate resonances of the polymer species of PVAQ from its monomeric residuals (Figure S2a). The polymer species of PVAQ are encoded in the 1D ¹H NMR spectra (Figure S1d) as two broad signals of approximately 1.5 ppm FWHM in the aromatic and aliphatic region of the spectrum respectively. On-top of these broad resonances the sharp resonances of the mobile monomeric species are

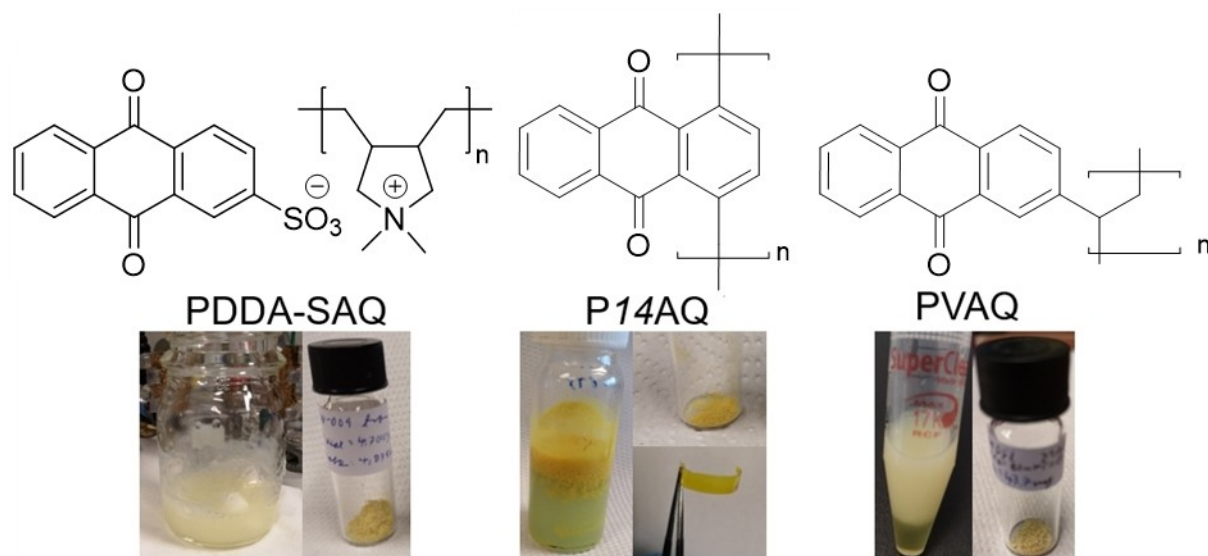


Figure 1. Chemical structures of PDDA-SAQ, P14AQ and PVAQ and images of the precipitated polymers as well as their powder form after drying and as a free-standing film for P14AQ.

visible. The broad solid-state like resonances of the polymer is an indication of the strongly hindered rotational motion of the polymer structures and the lack of any long-range order. A strong hindrance of internal rotation in the side-chain moieties of the polymer is indicated by the lack of structural modulation in the line shape of the aromatic resonances.

Furthermore, we can verify the pure polymeric form, with no monomeric residuals, for P14AQ (Figure S1a). The aromatic region of the 1D ^1H NMR spectrum of P14AQ shows a lower chemical shift dispersion as compared to PVAQ and four separate, broadened resonances can be identified. This can be explained by the larger rotational freedom of the aromatic side-chain moieties. Comparison of the $\log D_i$ values of polymeric P14AQ and PVAQ indicates slower diffusion of P14AQ, which is

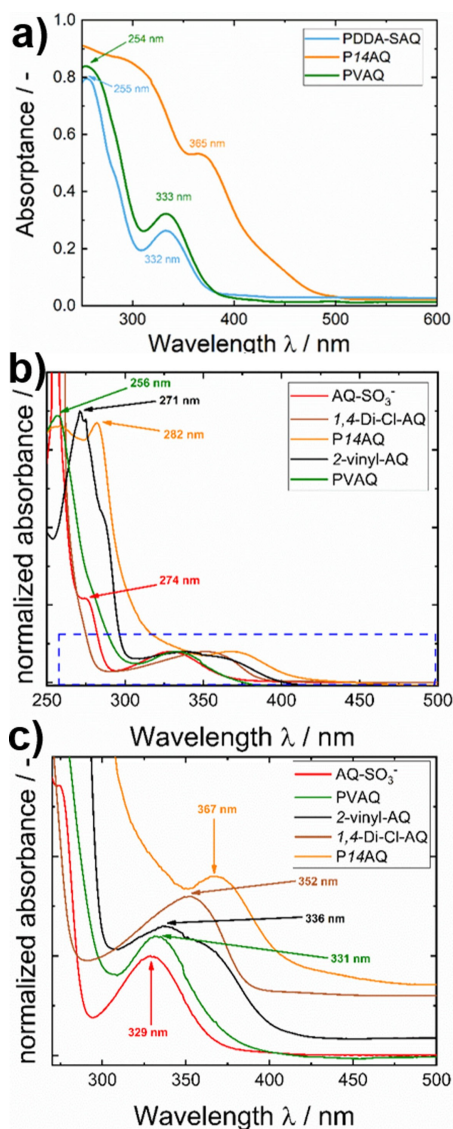


Figure 2. Absorbance spectra of thin-films of PDDA-SAQ, P14AQ and PVAQ a) quartz glass, b) and c) UV-Vis absorption spectra of P14AQ, PVAQ in CHCl_3 and the monomers AQS in H_2O and 1,4-Di-Cl AQ and 2-vinyl-AQ in CHCl_3 . Specific zoom area in c) is marked with a blue square and hereby the spectra were stacked with an offset for better visibility.

translated to a larger polymeric structural size of P14AQ than PVAQ.

UV-Vis absorption spectroscopy was performed on thin films of the three polymers deposited on quartz glass by blade coating as well as on solutions of P14AQ, PVAQ and the monomer species.

Polymer coated substrates show a pale-yellow colour of the P14AQ film, whereas in the case of PDDA-SAQ and PVAQ nearly no color changes were observed. This observation was proven by the thin-film absorbance measurements in Figure 2a, which showed that only P14AQ exhibited an absorption tail into the visible light regime above 400 nm. The direct comparison of solutions of the AQ monomers with the dissolved polymers P14AQ and PVAQ in Figure 2c revealed that in the case of PVAQ the polymer shows a slight hypsochromic shift of its absorption maximum at 331 nm compared to the monomer 2-vinyl-AQ at 336 nm. This nearly unchanged optical behavior agrees with the fact that upon the PVAQ polymerization, no extension in the π -conjugated system occurs. In contrast to this, dissolved P14AQ shows a strong bathochromic shift compared to the 1,4-di-chloro anthraquinone (1,4-Di-Cl-AQ) monomer with a maximum at 367 nm vs. 352 nm, which is in good agreement with literature reports.^[47] The measurement of the absorbance of the P14AQ thin-film revealed comparable absorption maxima values but an even stronger red-shift of the absorption tail in the regime of 500 nm indicating that upon film formation the π -conjugated system increases due to stacking. In case of PDDA-SAQ and PVAQ such high wavelength tails were not observed due to lack of intermolecular interactions of the AQ units, as expected.

Attenuated total reflection Fourier-transformed infrared (ATR-FTIR) spectra of the three prepared polymers are shown in Figure 3. The FTIR spectra show well-resolved vibration bands, which differ from the synthesis educts (See Figure S3 for the comparison with spectra of the educts) and are in good accordance with previous literature reports about PDDA-SAQ and P14AQ.^[26,45,47]

Thermal and Surface Characterization

The three investigated polymers and their monomers or in case of PDDA-SAQ, the precursor polymer known as poly(diallyldimethylammonium chloride) (PDADMAC), were analyzed by thermogravimetric analysis (TGA). The results are summarized in Table 1.

Table 1. Comparison of the compounds with respect to their decomposition temperature T_d and their weight loss between 100 and 600 °C.

Sample	T_d [°C]	Weight loss [%] (100–600 °C)
PDADMAC	358/447	99.2
PDDA-SAQ	343	46.9
1,4-Di-Cl-AQ	298	99.7
P14AQ	501	19.2
2-vinyl-AQ	416	79.7
PVAQ	389	74.4

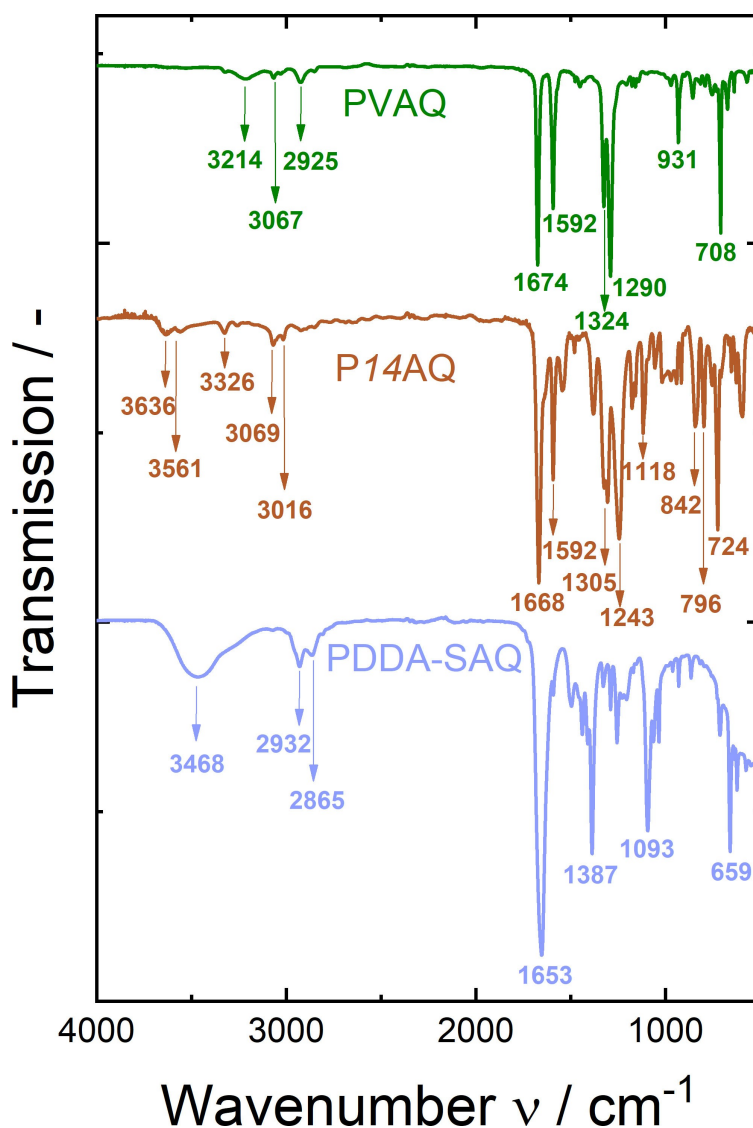


Figure 3. ATR-FTIR spectra of the three polymers PDDA-SAQ, P14AQ and PVAQ with the most prominent bands marked.

The full TGA graphs are reported in Figure S4. As can be seen from Table 1, the polymers PDDA-SAQ and PVAQ showed a similar or even a lower decomposition temperature (T_d) as their synthesis educts. In contrast, the polymer P14AQ showed high thermal stability with a decomposition temperature slightly above 500 °C, which conforms to literature reports.^[26] In the case of monomer 1,4-Di-Cl-AQ, the step and complete loss of weight at around 300 °C is most likely due to the sublimation of the compound. Besides the high decomposition temperature, the polymer P14AQ also showed the smallest weight loss of only 19% upon heating up to 600 °C in contrast to 47% and 74% for PDDA-SAQ and PVAQ, respectively. These results revealed a significantly higher thermal stability of the polymer P14AQ in comparison with PDDA-SAQ or PVAQ. This might be relevant for future investigations if industrially operated batteries or electrolyzers are required to run at elevated temperatures.^[52]

In order to examine the three polymers towards their hydrophilic or hydrophobic surface properties, the polymers were drop-casted onto glassy carbon (GC) and compared to bare GC with respect to their contact angle of a MilliQ water (MQ) drop, as illustrated in Figure 4.

The contact angle of bare GC was quite high, with 74.1°, which demonstrates a certain intrinsic hydrophobicity. This result is following literature.^[53] It has to be kept in mind, however that upon applying a potential the surface hydrophobicity can change.^[54] By the polarities of the side chains, the PDDA-SAQ film was rather hydrophilic, whereas the PVAQ film was slightly more hydrophobic than GC itself. The measured contact angle for the P14AQ film of 49.7° was significantly lower than expected, thus indicating a hydrophilic behavior from this polymer (see chemical structure in Figure 1).

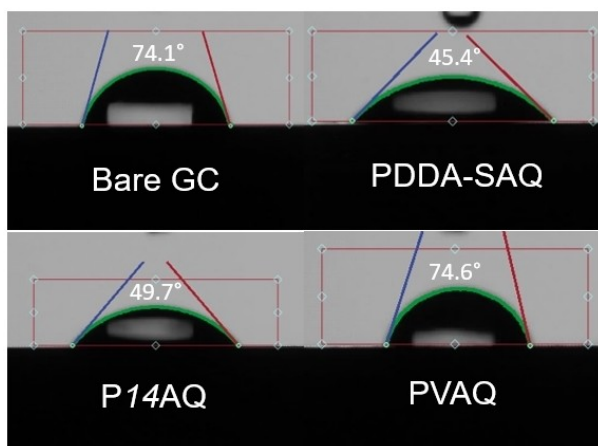


Figure 4. Contact angle measurements with MQ water on bare GC, PDDA-SAQ, P14AQ and PVAQ.

Electrochemical characterization

As outlined in the beginning, the goal of this work is to examine and derive trends for poly(antraquinones) for all kinds of energy storage applications. Nevertheless, as these polymers are already extensively studied for their battery performance, we have solely focused on basic electrochemical performance and electrocatalytic oxygen reduction. Zarren et al. reviewed several poly(antraquinones) and listed their specific capacity values.^[44] According to the review and the seminal papers, PDDA-SAQ shows a specific capacity of 130 mA h g^{-1} ,^[45] P14AQ 260 mA h g^{-1} ^[26] and PVAQ a specific capacity of above 200 mA h g^{-1} .^[49]

Electrochemical investigation of the three drop-casted thin-films of the three different AQ-based polymers was performed with cyclic voltammetry under both, inert nitrogen-saturated (N_2) conditions and oxygen-saturated (O_2) conditions. As mentioned above, organic electrocatalysts for the ORR are not only relevant for electrochemical H_2O_2 production, but also fuel cell or polymer-air battery application.

Cyclic voltammograms under N_2

Most of the reported CV studies for poly(antraquinones) in aqueous solutions are measured in alkaline electrolyte solutions. From a technical application point of view, the investigation of the materials under neutral conditions would be more favorable as the stability of H_2O_2 in solution decreases with increasing pH value. Thus, the cycle stabilities of the investigated polymers were measured by recording 50 CV cycles of each polymer in a 0.1 M phosphate buffer at pH = 7 (PB), as illustrated in Figure 5.

Figure 5 shows that PDDA-SAQ shows the largest faradaic current response of all three materials in PB, which is in agreement with the high ionic conductivity of such poly(ionic liquids).^[46] Nevertheless, the j_p of these peaks decays quite fast

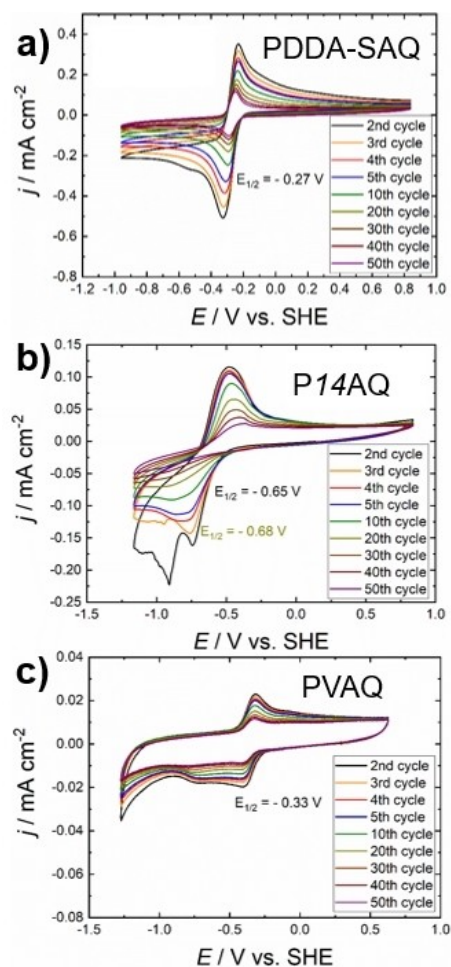


Figure 5. CV cycle stability graphs for a) PDDA-SAQ, b) P14AQ and c) PVAQ measured in 0.1 M PB at pH = 7.

with increasing cycle number, which indicates poor electrochemical cycle stability of the PDDA-SAQ in neutral solution.

In a 0.1 M NaOH solution shown in Figure 6 within the first 3 cycles the faradaic response of PDDA-SAQ was even higher compared to the PB, but the cycle stability was much worse and there were also some spike-shaped irregularities observed. These redox-peak shapes of the immobilized AQ units in the polymeric form are in good agreement with a previous study using a non-covalent immobilization approach onto carbon nanotubes.^[32] Besides a lower j_p , PVAQ also showed a quite rapid fading of the faradaic current response in neutral as well as alkaline solution. Interestingly, P14AQ showed a similar current fading behavior in neutral solution, but a nearly unchanged CV response in alkaline solution over 50 cycles. A possible explanation for this is the reported difference in ionic conductivities between OH^- and the phosphate anions as well as swelling properties of certain polymers.^[55] Similar behavior was recently reported regarding a proton-assisted metal-quinone intercalation mechanism.^[56]

The CV behavior in acidic solution at pH = 2 (See Figure S5b,d,f) revealed that only PDDA-SAQ is showing some redox behavior whereas P14AQ and PVAQ showed no faradaic

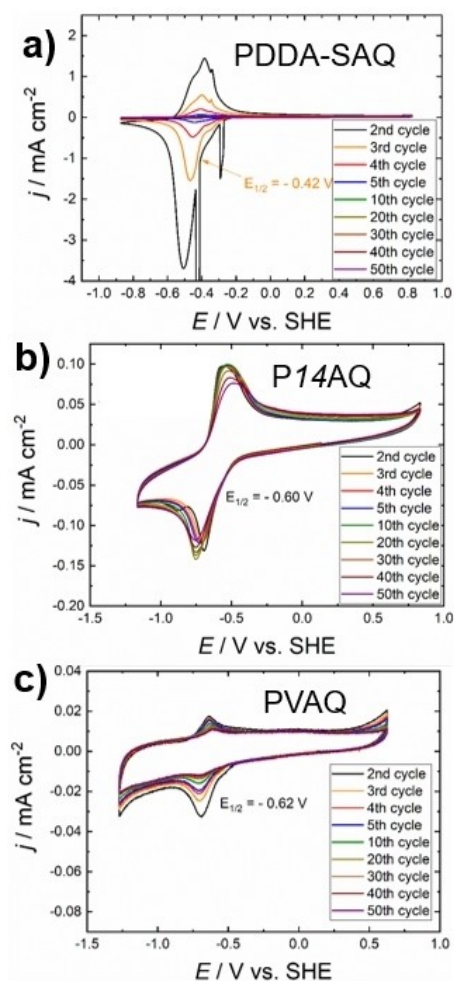


Figure 6. CV cycle stability graphs for a) PDDA-SAQ, b) P14AQ and c) PVAQ measured in 0.1 M NaOH at pH = 13.

current response at all. In order to check the high cycle stability of PVAQ proposed by Choi *et al.*^[49] also CV studies in 2.5 M NaCl at pH = 13 were performed (See Figure S5a,c,e). These experiments under a high ionic strength revealed increased cycle stability, faradaic current response as well as a sharper and more reversible peak shape in the case of P14AQ and PVAQ whereas in the case of PDDA-SAQ the reductive dissolution happened even faster as compared to 0.1 M NaOH.

Cyclic voltammogram comparison between N_2 and O_2

As Hernández *et al.*^[45] already proposed PDDA-SAQ as electrocatalyst for the oxygen reduction in alkaline media, the three polymers prepared in this work were also investigated for their possible electrocatalytic behavior, as illustrated in Figure 7.

As can be seen from Figure 7a, PDDA-SAQ showed an electrocatalytic feature in addition to the AQ peaks for the oxygen reduction compared to the bare GC electrode, which was in good agreement with the previous studies.^[45] In addition to a higher electrocatalytic current density, also the required

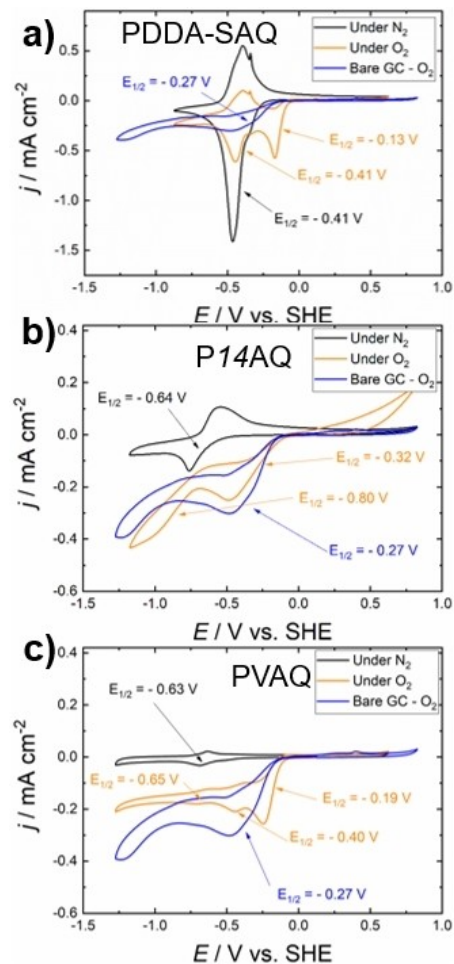


Figure 7. CV comparison of polymer-coated GC with bare GC in 0.1 M NaOH at pH = 13 under N_2 and O_2 saturated conditions. a) PDDA-SAQ, b) P14AQ and c) PVAQ.

potential for this oxygen reduction reaction was anodically shifted by 140 mV, in comparison to the bare GC. As PDDA-SAQ is the only one of these polymers with reversible redox-activity in neutral solution, it was also investigated towards electrocatalysis in 0.1 M PB, which demonstrated an analogous behavior like in alkaline solution (See Figure S6 for further information). In contrast to PDDA-SAQ, P14AQ did not show any sign for electrocatalysis, since the P14AQ coated GC showed lower j_p compared to the bare GC, with a similar cathodic shift. Figure 7c reveals that PVAQ yielded a lower j_p compared to bare GC, but still showed a small anodic shift of this oxygen reduction peak, the faint AQ redox-peak like under N_2 could be observed even under O_2 .

As a result of the cathodic shift and j_p reduction in the case of P14AQ and the j_p reduction together with fast reductive dissolution of PVAQ in alkaline media, only PDDA-SAQ could be referred to as an electrocatalyst for the oxygen reduction. Nevertheless, even in the case of PDDA-SAQ, the mentioned high cycle stability reported^[45] was not observed in alkaline media, which means that according to our findings, PDDA-SAQ

would act better as an immobilized electrocatalyst in neutral solutions. Therefore the previously discussed stability issue limits the application of such polymer-based immobilization techniques for aqueous oxygen reduction electrocatalysis. To prove that hypothesis, further in-depth studies would be required like chronoamperometry with detection of produced H_2O_2 or rotating ring-disc electrode investigations, which were not possible due to the aforementioned limited stability.

Scanning electron microscopy

To characterize the surface appearance of the investigated polymer films on GC, scanning electron microscopy (SEM) was used. Moreover, the as-casted films on GC were compared with the surface images of polymer films after 50 CV cycles performed in the medium of their best stability as illustrated in Figure 8.

As can be seen by eye as well as in Figure 8a, the initial PDDA-SAQ film was thicker and rougher in comparison to the other two polymers. Interestingly, after 50 electrochemical cycles, most of the polymer underwent reductive dissolution and only small polymer islands remained, which confirms the observations made during the CV measurements (see graphics in Figure 5a). Although the polymer P14AQ can be seen directly by the naked eye, the P14AQ film on GC can be hardly seen in the SEM images. This may be related to its apparently low electric conductivity and highly uniform and smooth surface. Therefore, the film made of P14AQ (right side, Figure 8c) was shown in contrast to a bare GC surface (left side, Figure 8c). Comparison of the SEM images of the film before and after CV cycle stability tests shows that the P14AQ film remains completely unchanged during CV cycling in 0.1 M NaOH. As can be seen in Figure 8e, the PVAQ film is also quite uniform, but shows a slight surface roughness. According to CV studies in

0.1 M PB in Figure 5e, PVAQ exhibited a more stable behavior, which was also underlined by just a slight increase in the surface morphology, but otherwise unchanged appearance upon CV cycle treatment.

Structure-property relations

As outlined in the beginning, the main goal of this work was to achieve a stable way of immobilizing redox-active molecules on electrodes while retaining all electrochemical benefits from homogeneously dissolved molecules. In order to obtain the relation between structure and properties, the results gained from different techniques were compared. Thus, electrochemical parameters were compared to the ones obtained by spectroscopic and surface hydrophilicity (contact angle) measurements. All the CV cycle studies done in the organic and aprotic solvent acetonitrile (MeCN) are shown in Figure S7.

The area between 2000 and 1500 cm^{-1} from ATR-FTIR spectra (Figure S8) are a close-up of the full spectra shown in Figure 3 and Figure S3. Figure 9 shows a plot of the wavenumber of carbonyl stretching vibration ($\nu_{\text{C=O}}$) and the hydrophobicity (expressed as contact angle θ) versus the measured potential in 0.1 M NaOH and MeCN like in Figure 9, one can deduce qualitative trends for further optimization of the immobilization pathways. Regarding the carbonyl vibration wavenumbers (black lines) one can clearly see a trend showing that polymers with a higher $\nu_{\text{C=O}}$ (which is equivalent to a stronger bond or spring constant via *Hooke's law*) require a more cathodic potential for the electrochemical reduction, in both alkaline aqueous solution and in acetonitrile solution. In addition to the molecular properties of the carbonyl bond, also intermolecular hydrogen bonds lower the $\nu_{\text{C=O}}$ significantly.^[57] We presume that the reason for this weaker $\nu_{\text{C=O}}$ considering the covalent polymers P14AQ and PVAQ is a result of an

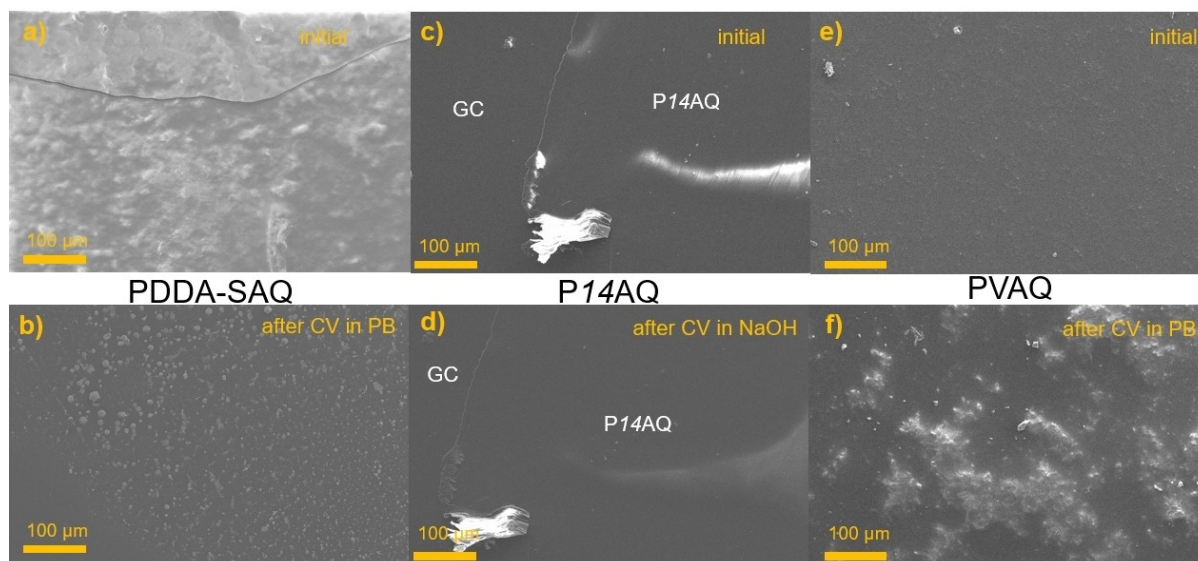


Figure 8. SEM images of the as-casted films of all three polymers before and after the CV cycling: PDDA-SAQ (a–b), P14AQ (c–d) and PVAQ (e–f) at different conditions as stated. In parts c and d the areas of GC and the ones covered with P14AQ are marked.

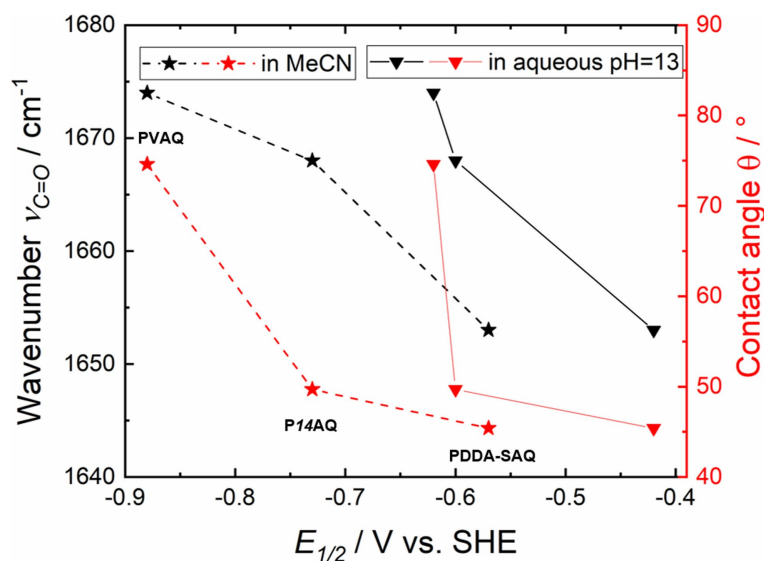


Figure 9. Relation of $\nu_{C=O}$ with $E_{1/2}$ and the hydrophobicity with $E_{1/2}$. The polymer attribution is given for the values determined in MeCN which are marked with *. The black lines refer to the $\nu_{C=O}$ whereas the red lines correspond to the θ values.

increased π -electron delocalization. Furthermore, comparison of the contact angle trend shows that a higher hydrophobicity of the polymers (larger θ value) relates to a more cathodic reduction potential in both alkaline aqueous and acetonitrile solution. Such linear correlations between hydrophobicity and the electrochemical reduction potential were already reported for other systems.^[58,59] Some reports explain this phenomenon by a change in reorganization energy whereas the work by Ma *et al.*^[60] reported a qualitative relation between the electrochemical behavior of redox-polymers and a so-called polymer-water affinity. Another visualization of these trends in addition to the current density within the first reduction peak vs. θ can be found in Figure S9.

From these studies, it could be shown that both weaker C=O bonds (reflected by lower $\nu_{C=O}$) and higher hydrophilicity (reflected by lower θ values) lead to more anodically shifted reduction potentials of the anthraquinone moieties within the polymeric structure. Finally, this leads to the general suggestion that not only the selection of pendant catalytic groups but also the type of incorporation into the polymeric backbone structure are crucial factors to be considered for identification of an optimal polymeric immobilization approach for redox-active groups, like anthraquinones. One key-parameter that should also be investigated in future studies is the hydrophilicity represented by the contact angle θ where high hydrophilicity facilitates a reversible electron transfer with sufficient current densities. A recent work by Ma *et al.*^[60] agreed with that conclusion by quantifying these polymer-water interactions and the electroreduction kinetics with the polarity of the linking unit between the polymer backbone and the redox-active unit (in their case 2,2,6,6-tetramethyl-1-piperidinyloxy (TEMPO)). Recently, Oka *et al.*^[61] reported a synthetically new approach for a poly(anthraquinone)-based battery material with an explicitly hydrophilic backbone chain. Their findings regarding an improved electron transfer reaction coupled with proton trans-

port throughout the polymer film as a result of the increased hydrophilicity of the polymeric backbone coincided with the findings presented here. The method presented herein by simply measuring the contact angle of the final polymer-GC sample we recommend for further redox-polymer studies. Furthermore, as this method can be more easily performed compared to the determination of hydrophobicity via polar-non-polar partition coefficient^[58,59] or determination of the mass uptake of water upon electrochemical reduction via quartz-crystal microbalance (QCMB) technique^[60] we recommend it for evaluation of already reported polymers. Thus the importance of hydrophobicity of electroactive material was demonstrated again which is not only important in the field of battery research^[62,63] but also crucial for electrocatalysis.^[64,65]

Conclusion

In this work, we prepared three different poly(anthraquinones) PDDA-SAQ, P14AQ and PVAQ. After thorough investigations of their thermal, spectroscopic as well as surface properties, these polymers were examined towards their possible application as polymer electrodes. Their structural properties are correlated to their electrochemical properties. These evaluations revealed that more hydrophilic polymers exhibit a more anodic reduction potential as well as larger faradaic currents in aqueous solutions. This behavior can be understood by the meaning of electrode wetting for electrochemical investigations as a faradic response of a polymer electrode does not only require the electron transfer but also sufficient counter ions for charge compensation provided by wetting and diffusion within the electrolyte solution. The second qualitative correlation was that the polymers exhibiting a more anodic reduction potential show a weaker C=O bond reflected by a lower wavenumber of the $\nu_{C=O}$, as determined by FTIR. This may originate from an

increased π -electron delocalization within a covalent poly(anthraquinone).

According to our findings, as well as those recently reported by Oka *et al.*,^[61] the following two key-aspects for the development of new poly(anthraquinones) for energy storage should be considered: i) The polymeric backbone should be on the one hand stable to prevent reductive dissolution but on the other hand also quite hydrophilic to allow sufficient wetting in aqueous solutions. ii) The anthraquinone units should be bound tightly enough in the polymer to prevent reductive dissolution but should also exhibit some spatial flexibility to allow sufficient electron and ion transport throughout the polymer thin film. In addition to the blunt molecular structure of poly(anthraquinones), further studies on how intermolecular interactions like e.g. hydrogen bonds that affect the electrochemical performance of redox-active polymers are recommended.

Experimental Section

Synthesis of PDDA-SAQ

Poly(diallyldimethyl ammonium sulfonic acid anthraquinone) (PDDA-SAQ) was synthesized according to a reported procedure.^[45] 50 mL of an aqueous solution of sodium anthraquinone sulfonate (25 mM in MQ water, TCI Chemicals) (AQS) were dissolved by sonication for 15 min. Poly(diallyldimethyl ammonium chloride) (500 μ L, 0.62 mmol, 20% in H₂O, Sigma-Aldrich, 200 000–350 000 g mol⁻¹) (PDADMAC) were diluted in MQ water (500 μ L) and stirred. To this PDADMAC solution, the AQS solution was added dropwise under vigorous stirring for 20 min. During this addition, the solution turned turbid and very viscous upon gelation. Afterward, this suspension was stirred for 3 h and subsequently left unstirred for 3 h more.

Then the polymer was filtered and washed with MQ water (5 mL \times 6) followed by vacuum drying at 50 °C for 6 h, yielding a dried yellow flake-like powder (yield ca. 70%).

Synthesis of P14AQ

Poly(1,4-anthraquinone) (P14AQ) was prepared according to the reported procedure through an organometallic condensation reaction by Yamamoto and Etori^[47] which was optimized by Song *et al.*^[26] 1,4-Dichloro-anthraquinone (83.1 mg, 0.30 mmol, TCI Chemicals) (1,4-Di-Cl-AQ) was weighed directly in a glass vial and flushed with nitrogen (N₂). Then, *N,N*-dimethyl formamide (DMF) (2 mL, VWR Chemicals) was added and the solution was stirred for 2 h, performed inside a glove box. In another glass vial, also under inert conditions inside the glove box, 2,2'-bipyridine (63.2 mg, 0.40 mmol, Sigma-Aldrich), bis(1,5-cyclooctadiene)nickel(0) (110.5 mg, 0.40 mmol, Alfa Aesar) and *cis,cis*-1,5-cyclooctadiene (37.0 μ L, 0.30 mmol, Alfa Aesar) were dissolved with DMF (3.0 mL, VWR Chemicals). The previously prepared anthraquinone solution was added to the 2nd vial, inside the glove box, and the reaction mixture was sealed. The reaction mixture was transferred outside of the glove box, kept under argon and heated, under stirring, at 60 °C for 48 h. After cooling down to room temperature (RT), the reaction was neutralized with hydrochloric acid (HCl) solution (10 mL, 0.5 M, Merck) and left unstirred for 30 min to sediment. The precipitated polymer was filtered by vacuum and washed: with DMF (5 mL \times 4), HCl (5 mL \times 5 of 0.5 M), MQ-water (5 mL \times 5) and finally with

methanol (5 mL \times 5, VWR Chemicals). The product was dried at RT overnight and re-dissolved in chloroform (CHCl₃) (3 mL, VWR Chemicals). Then, the polymer was precipitated with MeOH (10 mL) followed by filtration with vacuum and washed with MeOH (5 mL \times 3). The final P14AQ polymer was dried in vacuum at room temperature for 6 h, yielding a yellow powder (yield ca. 80%).

¹H-NMR (300 MHz, CDCl₃, δ /ppm): 8.21 (br, 1H), 8.11 (br, 1H), 7.91 (br, 2H), 7.73 (br, 2H).

Synthesis of PVAQ

Poly(2-vinylantraquinone) PVAQ was prepared from an adapted procedure reported in literature.^[49,50] Monomer 2-vinylantraquinone (93.7 mg, 0.4 mmol, Sigma-Aldrich) and initiator benzoyl peroxide (6.45 mg, 0.02 mmol, 5% initiator to monomer ratio (mol/mol), Merck) were dissolved in chloroform (5 mL, VWR Chemicals) in a Wheaton bottle. The Wheaton bottle was sealed and the reaction mixture was sonicated for 5 min, followed by degassing through for three vacuum/N₂ cycles. The reaction mixture was then stirred under a N₂ atmosphere and heated to 60 °C in an oil bath for 24 h. After that time, the solution was added to a centrifuge tube and the solvent was reduced to \sim 2 mL by evaporation under air. Then, the toluene was added (2 mL, VWR Chemicals) to let the product precipitated for 2 h. The product was purified by centrifugation and washed with toluene (2 mL \times 3, 5 min, at 5500 rpm). Finally, the polymer PVAQ was dried under vacuum (at 50 °C, 4 h) and further dried in a vial for 8 h at 60 °C, yielding a yellow-white powder (yield ca. 46%).

¹H-NMR (300 MHz, CDCl₃, δ /ppm): 8.43-7.30 (br, 7H, Ar), 2.43-1.58 (br, 3H).

Characterization methods

Normal ¹H-NMR spectra were recorded with 300 MHz, using a Bruker® Advance 300 spectrometer. For Diffusion ordered spectroscopy (DOSY) NMR, ¹H NMR spectra were recorded on a Bruker Avance III 500 spectrometer^[66] at a ¹H Larmor frequency of -500.13 MHz. ¹H chemical shifts are given in parts per million (ppm), are referenced to the used deuterated solvent, chloroform, and are recalculated to the TMS scale (δ C¹H₃, 0.0 ppm). 2D DOSY spectra were recorded using the Bruker topspin pulse sequence "dstebppg3s" for diffusion measurements.^[67,68] It uses double stimulated echo for convection compensation and a longitudinal eddy current delay (LED). Further, it uses bipolar gradient pulses for diffusion and 3 spoil gradients. The diffusion time Δ was 100 ms and the gradient pulse length δ was 1.5–2.0 ms. The diffusion gradient was incremented from 2–95% in 24–32 steps.

Thermogravimetric analyses were carried out with a TGA/PerkinElmer Q5000, with platinum pans and measurements between 50 and 900 °C, a heating rate of 10 °C min⁻¹ under nitrogen (25 mL min⁻¹).

The UV-Vis absorption studies for solutions were performed on a Varian Cary 3G UV-visible spectrophotometer using a 10 mm path length quartz cuvette.

UV-Vis transmittance and reflectance spectra were used to determine the spectral absorbance and were measured on a PerkinElmer Lambda 1050 spectrophotometer. For reflectance measurements, a 6° specular reflectance accessory was used. Polymer thin films for optical characterization were fabricated on quartz glass substrates by blade coating from 10 mg/mL solutions of the polymers in chloroform (P14AQ and PVAQ) or DMF (PDDA-SAQ), respectively. Blade coating deposition was carried out on an Erichsen Coatmaster 509 MC at speeds of 35–40 mm/s at room

temperature for chloroform solutions and at 115 °C for DMF solutions. Before deposition, quartz glass substrates were treated with an oxygen plasma at 100 W for 5 minutes in a Plasma Etch PE-25 plasma cleaner.

Attenuated total reflection Fourier-transform infrared spectroscopy (ATR-FTIR) was performed on a Bruker VERTEX 80-ATR spectrometer between 4000 and 500 cm⁻¹ averaging 64 scans.

Scanning electron microscopy (SEM) images of polymer films were recorded on a JEOL JSM-6360LV scanning electron microscope operated under high vacuum settings at an acceleration voltage of 7.0 kV.

The contact angle measurements were performed on an Ossila Contact Angle Goniometer at room temperature using MQ water.

Electrode preparation

In all electrochemical experiments, a 3 mm glassy carbon (GC) disc-type electrode (PalmSens) was used. Before modification with a polymer, the GC WE was polished for 30 s each with Buehler Micropolish II deagglomerated alumina with decreasing particle size from 1.0 to 0.3 and 0.05 μm. Between those polishing steps, excess alumina was removed via rinsing with MQ water and isopropanol (VWR Chemicals).

For electrochemical analysis of the three polymer samples, in all cases a 10 mg mL⁻¹ solution was prepared and sonicated for 2 h each. In case of P14AQ and PVAQ, chloroform (VWR Chemicals) was used as solvent while for PDDA-SAQ, DMF (VWR Chemicals) was used.

5 μL aliquots were drop-casted onto the GC WE and dried overnight in ambient conditions.

Electrochemical Experiments

For all electrochemical measurements, a Jaissle Potentiostat – Galvanostat PGU10 V-100 mA was used in a three-electrode configuration. A platinum plate (Pt) was used as the counter electrode (CE), a Ag/AgCl (3 M KCl) electrode (BASi) as a reference electrode (RE) and the (modified) GC as WE. For the determination of the current density (*j*), in all cases the geometric electrode area was considered.

Supporting Information

Supporting Information is available from the Wiley Online Library.

Acknowledgements

The authors gratefully acknowledge financial supports from the Austrian Science Foundation (FWF) within the Wittgenstein Prize for Prof. Sariciftci (Z222-N19).

NMR experiments were performed at the Upper Austrian-South Bohemian Research Infrastructure Center in Linz, co-financed by "RERI-uasb", EFRE RUZ-EU-124/100-2010 (ETC Austria-Czech Republic2007–2013, Project M00146).

We thank Paul Strasser and Maria Würflinger from the Institute of Polymer Chemistry (ICP) and Felix Leibetseder from the

Institute for Chemical Technology of Organic Materials (CTO) for technical support. The authors gratefully acknowledge the support of Prof. Christian Paulik for providing the experimental facilities of the CTO institute.

Conflict of Interest

The authors declare no conflict of interest.

Keywords: Anthraquinones · Electrochemistry · Energy conversion and Storage · Immobilization · Redox-active polymers

- [1] M. Irimia-Vladu, Y. Kanbur, F. Camaioni, M. E. Coppola, C. Yumusak, C. V. Irimia, A. Vlad, A. Operamolla, G. M. Farinola, G. P. Suranna, N. González-Benitez, M. C. Molina, L. F. Bautista, H. Langhals, B. Stadlober, E. D. Glowacki, N. S. Sariciftci, *Chem. Mater.* **2019**, *31*, 6315.
- [2] D. Larcher, J. M. Tarascon, *Nat. Chem.* **2015**, *7*, 19.
- [3] Z. Song, H. Zhou, *Energy Environ. Sci.* **2013**, *6*, 2280.
- [4] P. Novák, K. Müller, K. S. V. Santhanam, O. Haas, *Chem. Rev.* **1997**, *97*, 207.
- [5] B. Häupler, A. Wild, U. S. Schubert, *Adv. Energy Mater.* **2015**, *5*, 1.
- [6] M. Miroshnikov, K. P. Divya, G. Babu, A. Meiyazhagan, L. M. Reddy Arava, P. M. Ajayan, G. John, *J. Mater. Chem. A* **2016**, *4*, 12370.
- [7] A. Pron, P. Gawrys, M. Zagorska, D. Djurado, R. Demadrille, *Chem. Soc. Rev.* **2010**, *39*, 2577.
- [8] Q. Zhao, A. K. Whittaker, X. S. Zhao, *Materials* **2018**, *11*, 2567.
- [9] C. Han, H. Li, R. Shi, T. Zhang, J. Tong, J. Li, B. Li, *J. Mater. Chem. A* **2019**, *7*, 23378.
- [10] B. K. Sharma, S. Dixit, S. Chacko, R. M. Kamble, N. Agarwal, *Eur. J. Org. Chem.* **2017**, *2017*, 4389.
- [11] Y. Liang, Y. Yao, *Joule* **2018**, *2*, 1690.
- [12] D. Werner, D. H. Apaydin, E. Portenkirchner, *Batteries & Supercaps* **2018**, *1*, 160; *Supercaps* **2018**, *1*, 160.
- [13] D. Werner, D. H. Apaydin, D. Wielend, K. Geistlinger, W. D. Saputri, U. J. Griesser, E. Drazevic, T. S. Hofer, E. Portenkirchner, *J. Phys. Chem. C* **2021**, *125*, 3745.
- [14] S. Gentil, D. Reynard, H. H. Girault, *Curr. Opin. Electrochem.* **2020**, *21*, 7.
- [15] B. Yang, L. Hooper-Burkhardt, F. Wang, G. K. Surya Prakash, S. R. Narayanan, *J. Electrochem. Soc.* **2014**, *161*, A1371.
- [16] N. An, Y. An, Z. Hu, Y. Zhang, Y. Yang, Z. Lei, *RSC Adv.* **2015**, *5*, 63624.
- [17] S. Ryu, E. Kim, J. Yoo, *Electrochim. Acta* **2021**, *370*, 137809.
- [18] D. S. Achilleos, T. A. Hatton, *ACS Appl. Mater. Interfaces* **2016**, *8*, 32743.
- [19] B. Gurkan, F. Simeon, T. A. Hatton, *ACS Sustainable Chem. Eng.* **2015**, *3*, 1394.
- [20] S. Voskian, T. A. Hatton, *Energy Environ. Sci.* **2019**, *12*, 3530.
- [21] D. Wielend, D. H. Apaydin, N. S. Sariciftci, *J. Mater. Chem. A* **2018**, *6*, 15095.
- [22] F. Mirkhalaf, K. Tammeveski, D. J. Schiffrin, *Phys. Chem. Chem. Phys.* **2004**, *6*, 1321.
- [23] Q. Li, C. Batchelor-McAuley, N. S. Lawrence, R. S. Hartshorne, R. G. Compton, *Chem. Commun.* **2011**, *47*, 11426.
- [24] D. Wielend, H. Neugebauer, N. S. Sariciftci, *Electrochem. Commun.* **2021**, *125*, 106988.
- [25] N. Casado, G. Hernández, H. Sardon, D. Mecerreyes, *Prog. Polym. Sci.* **2016**, *52*, 107.
- [26] Z. Song, Y. Qian, M. L. Gordin, D. Tang, T. Xu, M. Otani, H. Zhan, H. Zhou, D. Wang, *Angew. Chem. Int. Ed.* **2015**, *54*, 13947.
- [27] C. Guo, K. Zhang, Q. Zhao, L. Pei, J. Chen, *Chem. Commun.* **2015**, *51*, 10244.
- [28] X. Han, C. Chang, L. Yuan, T. Sun, J. Sun, *Adv. Mater.* **2007**, *19*, 1616.
- [29] Z. Lei, W. Wei-kun, W. An-bang, Y. Zhong-bao, C. Shi, Y. Yu-sheng, *J. Electrochem. Soc.* **2011**, *158*, A991.
- [30] Z. Gong, G. Zhang, S. Wang, *J. Chem.* **2013**, *2013*, 756307.
- [31] M. Mooste, E. Kibena-Pöldsepp, L. Matisen, K. Tammeveski, *Electroanalysis* **2017**, *29*, 548.
- [32] D. Wielend, M. Vera-Hidalgo, H. Seelajaroen, N. S. Sariciftci, E. M. Pérez, D. R. Whang, *ACS Appl. Mater. Interfaces* **2020**, *12*, 32615.

- [33] A. Wu, E. C. Venancio, A. G. MacDiarmid, *Synth. Met.* **2007**, *157*, 303.
- [34] C. Strietzel, M. Sterby, H. Huang, M. Strømme, R. Emanuelsson, M. Sjödin, *Angew. Chem. Int. Ed.* **2020**, *59*, 9631.
- [35] K. Oka, C. Strietzel, R. Emanuelsson, H. Nishide, K. Oyaizu, M. Strømme, M. Sjödin, *ChemSusChem* **2020**, *13*, 2280.
- [36] I. C. Monge-Romero, M. F. Suárez-Herrera, *Synth. Met.* **2013**, *175*, 36.
- [37] J. J. Leung, J. A. Vigil, J. Warnan, E. E. Moore, E. Reisner, *Angew. Chem.* **2019**, *131*, 7779.
- [38] E. Portenkirchner, J. Gasiorowski, K. T. Oppelt, S. Schlager, C. Schwarzhinger, H. Neugebauer, G. Knör, N. S. Sariciftci, *ChemCatChem* **2013**, *5*, 1790.
- [39] D. H. Apaydin, E. Tordin, E. Portenkirchner, G. Aufischer, S. Schlager, M. Weichselbaumer, K. T. Oppelt, N. S. Sariciftci, *ChemistrySelect* **2016**, *6*, 1156.
- [40] J. Luangchaiyaporn, D. Wielend, D. Solonenko, H. Seelajaroen, J. Gasiorowski, M. Monecke, G. Salvan, D. R. T. Zahn, N. S. Sariciftci, P. Thamyongkit, *Electrochim. Acta* **2020**, *367*, 137506.
- [41] H. Rabl, D. Wielend, S. Tekoglu, H. Seelajaroen, H. Neugebauer, N. Heitzmann, D. H. Apaydin, M. C. Scharber, N. S. Sariciftci, *ACS Appl. Energ. Mater.* **2020**, *3*, 10611.
- [42] P. M. Hoang, S. Holdcroft, B. L. Funt, *J. Electrochem. Soc.* **1985**, *132*, 2129.
- [43] M.-C. Pham, J.-E. Dubois, *J. Electroanal. Chem.* **1986**, *199*, 153.
- [44] G. Zarren, B. Nisar, F. Sher, *Mater. Today Sustain.* **2019**, *5*, 100019.
- [45] G. Hernández, M. Isik, D. Mantione, A. Pendashteh, P. Navalotro, D. Shanmukaraj, R. Marcilla, D. Mecerreyes, *J. Mater. Chem. A* **2017**, *5*, 16231.
- [46] A. S. Shaplov, R. Marcilla, D. Mecerreyes, *Electrochim. Acta* **2015**, *175*, 18.
- [47] T. Yamamoto, H. Etori, *Macromolecules* **1995**, *28*, 3371.
- [48] Y. Li, L. Liu, C. Liu, Y. Lu, R. Shi, F. Li, J. Chen, *Chem* **2019**, *5*, 2159.
- [49] W. Choi, D. Harada, K. Oyaizu, H. Nishide, *J. Am. Chem. Soc.* **2011**, *133*, 19839.
- [50] C. Clausen, E. Drazevic, A. S. Andersen, M. L. Henriksen, M. Hinge, A. Bienten, *ACS Appl. Energ. Mater.* **2018**, *1*, 243.
- [51] P. Groves, *Polym. Chem.* **2017**, *8*, 6700.
- [52] N. Wang, X. Dong, B. Wang, Z. Guo, Z. Wang, R. Wang, X. Qiu, Y. Wang, *Angew. Chem. Int. Ed.* **2020**, *59*, 14577.
- [53] Y. Zou, A. S. Walton, I. A. Kinloch, R. A. W. Dryfe, *Langmuir* **2016**, *32*, 11448.
- [54] D. J. Lomax, P. Kant, A. T. Williams, H. V. Patten, Y. Zou, A. Juel, R. A. W. Dryfe, *Soft Matter* **2016**, *12*, 8798.
- [55] J. Lopez, D. G. Mackanic, Y. Cui, Z. Bao, *Nat. Rev. Mater.* **2019**, *4*, 312.
- [56] C. Han, H. Li, Y. Li, J. Zhu, C. Zhi, *Nat. Commun.* **2021**, *12*, 2400.
- [57] Z. Lin, H. Y. Shi, L. Lin, X. Yang, W. Wu, X. Sun, *Nat. Commun.* **2021**, *12*, 4424.
- [58] P. Hosseinzadeh, Y. Lu, *Biochim. Biophys. Acta Bioenerg.* **2016**, *1857*, 557.
- [59] D. K. Garner, M. D. Vaughan, H. J. Hwang, M. G. Savelieff, S. M. Berry, J. F. Honek, Y. Lu, *J. Am. Chem. Soc.* **2006**, *128*, 15608.
- [60] T. Ma, A. D. Easley, S. Wang, P. Flouda, J. L. Lutkenhaus, *Cell Reports Phys. Sci.* **2021**, *2*, 100414.
- [61] K. Oka, S. Murao, M. Kataoka, H. Nishide, K. Oyaizu, *Macromolecules* **2021**, *54*, 4854.
- [62] Y. Chen, H. Wang, S. Ji, B. G. Pollet, R. Wang, *J. Ind. Eng. Chem.* **2019**, *71*, 284.
- [63] M. C. Schulze, G. M. Carroll, T. R. Martin, K. Sanchez-Rivera, F. Urias, N. R. Neale, *ACS Appl. Energ. Mater.* **2021**, *4*, 1628.
- [64] G. Xia, Y. Tian, X. Yin, W. Yuan, X. Wu, Z. Yang, G. Yu, Y. Wang, M. Wu, *Appl. Catal. B* **2021**, *299*, 120655.
- [65] D. Wakerley, S. Lamaison, F. Ozanam, N. Menguy, D. Mercier, P. Marcus, M. Fontecave, V. Mougél, *Nat. Mater.* **2019**, *18*, 1222.
- [66] *Topspin*, Bruker BioSpin GmbH, Rheinstetten, Germany, **2012**.
- [67] A. Jerschow, N. Müller, *J. Magn. Reson.* **1996**, *123*, 222.
- [68] A. Jerschow, N. Müller, *J. Magn. Reson.* **1997**, *125*, 372.

Manuscript received: September 30, 2021

Revised manuscript received: October 25, 2021

Accepted manuscript online: October 27, 2021